Publications of the Astronomical Society of the Pacific, **125**:1304–1314, 2013 November

An Investigation of the Use of Synthetic Spectra to Find the Ages of Stellar Clusters

Randa S. Asa'd[1]

Physics Department, American University of Sharjah, P.O. Box 26666, Sharjah, UAE Physics Department, University of Cincinnati, P.O. Box 210011 Cincinnati, OH 45221; raasad@aus.edu

M. M. Hanson

Physics Department, University of Cincinnati, P.O. Box 210011 Cincinnati, OH 45221; margaret.hanson@uc.edu

Andrea V. Ahumada[2]

Observatorio Astronómico de la Universidad Nacional de Córdoba, Argentina Consejo Nacional de Investigaciones Científicas y Tecnológicas (CONICET), Argentina; andrea@oac.uncor.edu

Received 2013 May 04; accepted 2013 September 18; published 2013 November 20

ABSTRACT. The utility of stellar cluster aging methods based on integrated spectra is clearly demonstrated by its extensive use by researchers for decades. However, few studies have determined the accuracy of such methods using a significant sample of age-calibrated stellar clusters with recent models. We have amassed a sample of 27 stellar clusters, 20 with new spectra we obtained with the SOAR and Blanco 4-m Telescopes, with previously determined ages using color-magnitude diagrams (CMDs). We compared the CMD ages to ages obtained from the clusters' integrated spectra. We find that the integrated spectra in the wavelength range 3626–6230 Å, when compared with high resolution computational models, provide very good age predictions. In particular, the spectral method is more robust in resolving the age-extinction degeneracy that plagues broad-band photometric aging methods. We observe no significant difference in the ability of the synthetic spectra to fit and properly age stellar clusters based on the intrinsic mass of the stellar clusters in our sample.

Online material: color figures

1. INTRODUCTION

The formation history of a galaxy can be revealed by knowing the ages of its star clusters. The need for accurate ages of star clusters is thus crucial in order to derive the correct details of the formation history of a galaxy (Trancho et al. 2007). Periodic assessment of traditional aging methods is important as improved data and stellar evolution models become available. This paper investigates the accuracy of current methods based on integrated spectra to obtain the age of stellar clusters.

As our calibration sources, we selected stellar clusters from The Large Magellanic Cloud (LMC) galaxy. The LMC is an excellent place to test different age determination methods of star clusters because it is close enough that the stars can be resolved in its clusters, but far away enough so that the whole cluster can also be observed as a single object with integrated light. Although the color-magnitude diagram (CMD) method of obtaining ages of resolved clusters is not absolute because of the significant differences in evolutionary models by the Geveva group (Lejeune & Schaerer 2001) and the Padova group (Marigo et al. 2008), it is in general the most accurate relative method for determining the ages of stellar clusters (Leonardi & Rose 2003; Wolf et al. 2007). For this reason we have selected a sample of LMC stellar clusters that have been previously aged based on a full CMD analysis from the literature to test the precision and accuracy of other less-reliable, but often-used methods to age stellar clusters.

In a previous paper (Asa'd & Hanson 2012, hereafter Paper 1), we examined the relation between the CMD age of 84 LMC stellar clusters and their age as determined by integrated photometry and found it to be only weakly correlated. In this contribution, we will examine the relation between the CMD age of a subset of our LMC calibration cluster sample and ages derived from integrated spectroscopy.

A number of methods have been used by researchers to derive the age of stellar clusters using integrated spectra. One way examines specific spectral features and derives the cluster age based on the strength of these features (Worthey & Ottaviani

[1] Visiting astronomer, Cerro Tololo Inter-American Observatory, National Optical Astronomy Observatory, which are operated by the Association of Universities for Research in Astronomy, under contract with the National Science Foundation. The SOAR Telescope is a joint project of Conselho Nacional de Pesquisas Cientificas e Tecnologicas CNPq-Brazil, The University of North Carolina at Chapel Hill, Michigan State University, and the National Optical Astronomy Observatory.

[2] This work was started while an ESO Fellow.

1997; Beasley et al. 2002). Another method uses ratios of different spectral features (Leonardi & Rose 2003). A third method fits the full observed spectrum to model spectra (Koleva et al. 2008; Cid Fernandes & Gonzalez Delgado 2010). There are two main types of integrated spectra models. The first is based on theoretically-computed spectra as will be discussed in § 3. The second is based on template spectra obtained directly from clusters of known age (Bica et al. 1990; Santos et al. 1995; Piatti et al. 2002). In this paper, we will fit the full integrated spectrum to computational models. Using the full spectrum lessens the influence of bad pixels that might be present at strategic spectral features. It further enables us to make use of all the spectral lines in the range as well as the continuum to constrain both age and reddening at the same time (Bica & Alloin 1986, 1987; Bica et al. 1990, 1994; Santos et al. 1995; Piatti et al. 2002, 2005; Santos et al. 2006; Palma et al. 2008; Talavera et al. 2010; Benítez-Llambay et al. 2012).

In § 2 we describe our new spectral data. In § 3 we provide details about the model synthetic spectra used for obtaining the stellar cluster ages. In § 4 we describe the method used for matching observed spectra to model spectra. In § 5 we apply our method to LMC stellar cluster spectra taken from the literature. We provide a similar test of our cluster spectra using FISA, the software package presented by Benítez-Llambay et al. (2012) in § 6. We present our analysis of the reliability of spectral aging methods in § 7. We summarize the results of our analysis in § 8.

2. THE NEW SPECTRAL DATA

The new spectral data used in this study were obtained in two observing runs: 6 nights in February 2011 with the RC spectrograph on the 4 m Blanco telescope on Cerro Tololo (Chile), and 4 nights in December 2011 with the Goodman spectrograph on the SOAR (SOuthern Astrophysical Research) telescope on Cerro Pachon (Chile). Our plan was to observe the full sample of 84 clusters given in Asa'd & Hanson (2012) but we only obtained spectra for a total of 20 clusters due to bad weather conditions during both runs.

We obtained integrated spectra by scanning the cluster with the slit starting on the southern edge, with the slit aligned east-west. Clusters were guided in right ascension at the sidereal rate. However, each cluster was guided in declination at a nonsidereal rate, based on the cluster diameter and the total exposure time desired. The challenge in scanning across the face of a stellar cluster is to decide what to call the "edges" of each cluster. Figure 1 shows the region included in each cluster observed with SOAR. We needed to focus on the central region of the cluster, as very little flux is coming from the outer stars (north and south). More importantly, the influence of field stars, not part of the cluster, will begin to influence the spectrum beyond this edge. For the clusters observed with the Blanco 4 m telescope the acquisition images are not available.

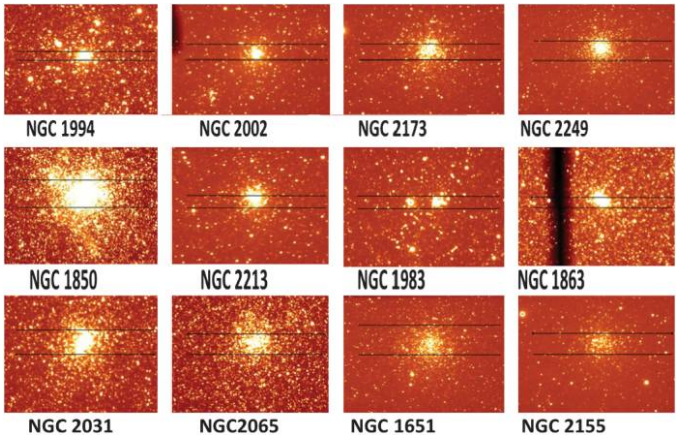

FIG. 1.—The region observed in each cluster in the SOAR run. The horizontal lines represent the slit position. (*north is up, east is to the left*). We stayed fairly close to the center of the cluster to avoid increasing field star contamination in the outer cluster regions. See the electronic edition of the *PASP* for a color version of this figure.

Table 1 shows the targets observed. Tables 2 and 3 give more information about each target and the time and speed of the scanning with the slit range. Table 2 shows the Blanco clusters and Table 3 shows the SOAR targets.

It was our goal to cover a broad range of ages and masses. We give special attention to cluster mass in our sample. Popescu & Hanson (2010) show that stellar clusters with masses below 10^5 solar masses are not able to fully populate the mass function, particularly at high mass. This leads to increasingly large stochastic variations in the integrated properties as mass decreases. Virtually all aging methods compare their observations to computational models that assume a fully populated mass function. In order to identify the increasing influence of stochastic effects with lower cluster mass in our sample, we categorize the clusters based on mass as introduced in Paper 1. Category 1 represents clusters with masses from 1,000 to $3,750\ M_{\odot}$. Category 2 represents clusters with mass from 3,750 to $10,000\ M_{\odot}$ Category 3 represents clusters with masses between 10,000 and $25,000\ M_{\odot}$. Category 4 represents clusters with masses between 25,000 and $100,000\ M_{\odot}$. Category 5 represents clusters with masses between 100,000 and $250,000\ M_{\odot}$. Figures 2, 3 and 4 show the distribution of cluster characteristics (age, mass and extinction) for our observed sample.

We reduced our data using the Image Reduction and Analysis Facility (IRAF)[3] in the usual manner. First, a bias image was subtracted from each raw image. A high signal-to-noise ratio (S/N), normalized flat field image was created, using a standard quartz lamp. This was divided from each of our target spectral images to correct for pixel-to-pixel sensitivity variations across

[3] IRAF is distributed by the National Optical Astronomy Observatory, which is operated by the Association of Universities for Research in Astronomy (AURA) under cooperative agreement with the National Science Foundation.

TABLE 1
TARGETS OBSERVED

Name	Run	Resolution (Å)	S/N	Mass[a]	Age[b]	Reference	E(B-V)	Reference
NGC1711	Blanco	14	118	4	7.4	Elson (1991)	0.16	Persson et al. (1983)
NGC1856	Blanco	14	67	4	7.90	Hodge (1984)	0.21	Kerber et al. (2007)
NGC1903	Blanco	14	28	2	7.85	Vallenari et al. (1998)	0.16	Vallenari et al. (1998)
NGC1984	Blanco	14	54	2	6.85	Hodge (1983)	0.14	Meurer et al. (1990)
NGC2011	Blanco	14	46	1	6.78	Hodge (1983)	0.08	Meurer et al. (1990)
NGC2156	Blanco	14	49	3	7.78	Hodge (1983)	0.1	Persson et al. (1983)
NGC2157	Blanco	14	79	4	7.6	Elson (1991)	0.10	Persson et al. (1983)
NGC2164	Blanco	14	98	4	7.7	Hodge (1983)	0.1	Persson et al. (1983)
NGC1651	SOAR	3.6	4	4	9.30	Mould et al. (1986a)	0.09	Mould et al. (1986a)
NGC1850	SOAR	3.6	22	4	7.60	Hodge (1983)	0.18	Alcaino & Liller (1987)
NGC1863	SOAR	3.6	21	3	7.76	Alcaino & Liller (1987)	0.2	Alcaino & Liller (1987)
NGC1983	SOAR	3.6	16	3	6.90	Hodge (1983)	0.09	Meurer et al. (1990)
NGC1994	SOAR	3.6	49	2	6.86	Hodge (1983)	0.14	Meurer et al. (1990)
NGC2002	SOAR	3.6	18	3	7.2	Elson (1991)	0.12	Persson et al. (1983)
NGC2031	SOAR	3.6	9	4	8.2	Dirsch et al. (2000)	0.09	Dirsch et al. (2000)
NGC2065	SOAR	3.6	33	3	7.85	Hodge (1983)	0.18	Persson et al. (1983)
NGC2155	SOAR	3.6	10	4	9.4	Elson & Fall (1988)	0.02	Kerber et al. (2007)
NGC2173	SOAR	3.6	7	5	9.32	Mould et al. (1986b)	0.14	Mould et al. (1986b)
NGC2213	SOAR	3.6	7	4	8.95	Da Costa et al. (1985)	0.09	Da Costa et al. (1985)
NGC2249	SOAR	3.6	7	4	8.82	Jones (1987)	0.01	Kerber et al. (2007)

[a] See the text for details about the mass ranges represented by these numbers.
[b] These are the CMD ages obtained from the literature. The unit is log(age/yr).

the detector. The illuminated portion of the spectral image is then converted into a one-dimensional spectrum by integrating the flux along the spatial direction of the two-dimensional image.

For the Blanco run the slit width was 3″. For the SOAR run we used a 1.3″ slit. The wavelength calibration was done using HeNeAr lamps for the Blanco run and HgAr lamps for the SOAR run. EG21 and CD32 were used as the standard photometric stars to calibrate the flux (Hamuy et al. 1992, 1994). Once the wavelength and flux calibration was completed and bad pixels identified, we combined the spectra of the clusters that were observed more than once to increase S/N in the final spectrum.

The wavelength range observed with the Blanco run is 3503–7244 Å with a resolution of 14 Å. For the SOAR data, we observed over a smaller range, 3625–6232 Å, but with a higher resolution of 3.6 Å. For consistent combined analysis we will be using the wavelength range of 3626–6230 Å for all clusters.

The flux was normalized to 1.00 at $\lambda = 5870$ Å where no critical spectral features are present. This was so the spectra

TABLE 2
BLANCO RUN (2011 FEBRUARY)

Name	Diameter	Exp. Time (min)	Speed
NGC1984	26″	50	7.2″/hr
NGC1984	26″	25	5.4″/hr
NGC1984	26″	5	5.4″/hr
NGC1856	24″	15	5.04″/hr
NGC2011	16″	60	3.6″/hr
NGC2011	16″	60	3.6″/hr
NGC2164	35″	30	68.4″/hr
NGC2164	35″	30	68.4″/hr
NGC2157	39″	45	25.2″/hr
NGC2157	39″	45	25.2″/hr
NGC1711	32″	45	46.8″/hr
NGC1711	32″	45	43.2″/hr
NGC2156	35″	45	50.4″/hr
NGC2156	35″	45	50.4″/hr
NGC1903	31″	45	43.2″/hr

TABLE 3
SOAR RUN (2011 DECEMBER)

Name	Diameter	Exp. Time (min)	Speed
NGC1994	18″	30	36″/hr
NGC2002	32″	20	48″/hr
NGC2173	32″	30	64″/hr
NGC2173	32″	30	64″/hr
NGC2249	38.7″	40	58″/hr
NGC1850	56″	30	112″/hr
NGC2213	24″	30	48″/hr
NGC2213	24″	30	48″/hr
NGC1983	19″	15	76″/hr
NGC1863	20″	30	40″/hr
NGC2031	50″	30	100″/hr
NGC2065	42″	20	84″/hr
NGC1651	62″	30	124″/hr
NGC1651	62″	30	124″/hr
NGC2155	42″	40	63″/hr
NGC2155	42″	40	63″/hr
NGC2155	42″	40	63″/hr

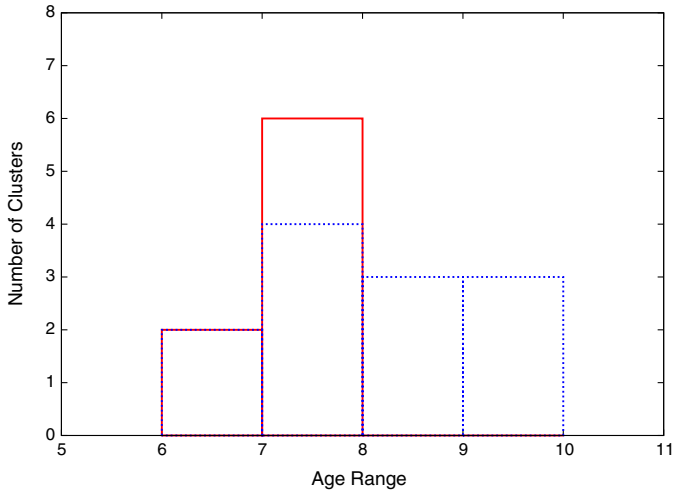

FIG. 2.—The distribution of log(age/year), for the sample observed with the Blanco telescope represented by the red (*continuous*) boxes and the clusters observed with SOAR telescope represented by the blue (*dotted*) boxes. It was our goal to cover a broad range of ages. See Tables 1 and 2 for more details. See the electronic edition of the *PASP* for a color version of this figure.

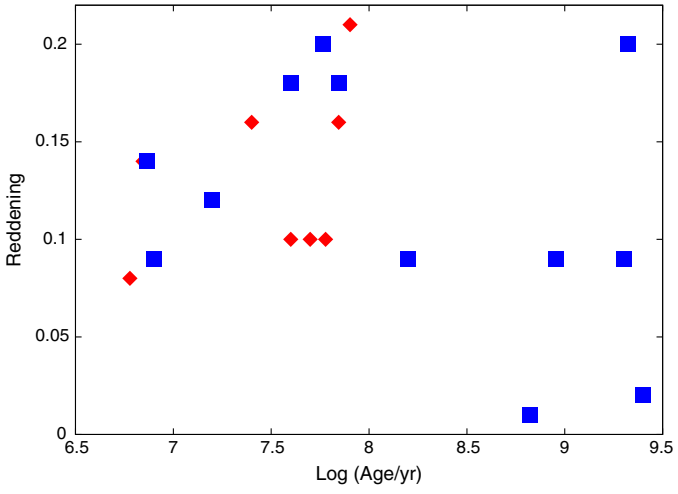

FIG. 4.—The extinction-age space of data obtained from literature for the clusters observed with Blanco represented by the red diamonds and the clusters observed with SOAR telescope represented by the blue squares. It was our goal to cover a broad range of extinctions. See Tables 1 and 2 for more details. See the electronic edition of the *PASP* for a color version of this figure.

can more easily be compared with the theoretical models. Both telescopes have about the same collecting area (4-m class). However, the Blanco spectra have on average much higher S/N per pixel compared to the SOAR spectra, as the slit was more than twice the width, and the resolution almost 4x lower. Also, we needed to push our SOAR observations to include much older clusters from our sample. These clusters were among the dimmest in our observed sample, again leading to some rather low S/N spectra from SOAR in a few cases.

Figures 5 and 6 show the spectra of clusters observed with Blanco and SOAR, respectively.

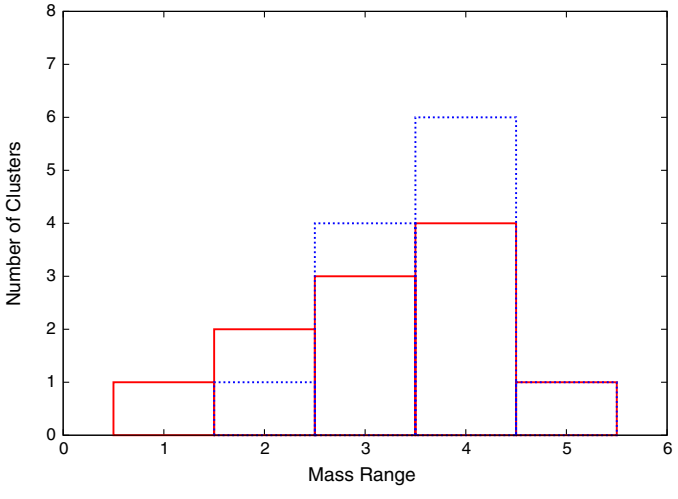

FIG. 3.—The distribution of masses (see the text for details about the definition of mass ranges) for the sample observed with the Blanco telescope represented by the red (*continuous*) lines and the clusters observed with SOAR telescope represented by the blue (*dotted*) lines. It was our goal to cover a broad range of masses. See Tables 1 and 2 for more details. See the electronic edition of the *PASP* for a color version of this figure.

3. INTEGRATED SPECTRA MODELS

As mentioned in § 1, integrated spectra have been used by researchers in a number of different ways to obtain the age and reddening of a stellar cluster. One popular method uses spectral templates (Bica et al. 1990; Santos et al. 1995; Piatti et al. 2002) which were created from real observations of clusters with

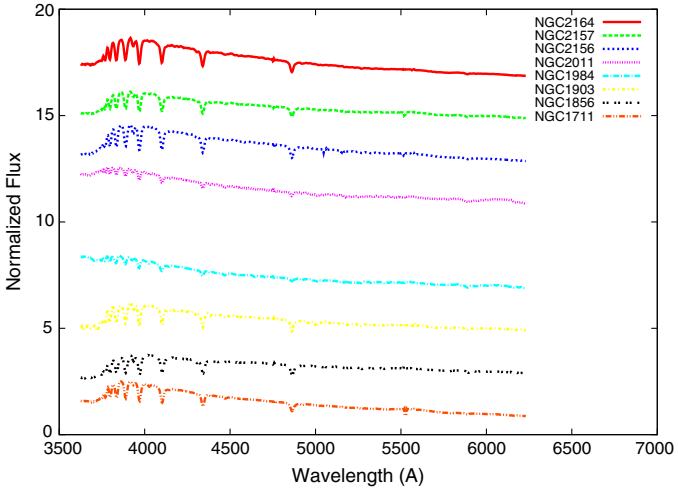

FIG. 5.—Spectra of the clusters observed with Blanco normalized at 5870 Å. The spectra are shifted on the vertical axis for clarity. See the electronic edition of the *PASP* for a color version of this figure.

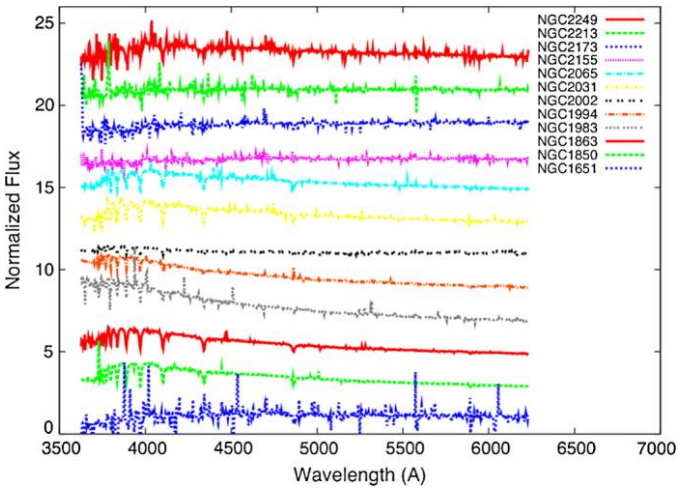

FIG. 6.—Spectra of the clusters observed with SOAR normalized at 5870 Å. The spectra are shifted on the vertical axis for clarity. See the electronic edition of the *PASP* for a color version of this figure.

known age and extinction properties. In our analysis, we will fit stellar ages using theoretically computed high-resolution (0.3 Å) synthetic spectra. The reasons for this are twofold. First, the templates originate from older studies where the spectral resolution was rather low compared to our new SOAR spectra. And second, the theoretical models provide a much larger range of cluster ages to compare against our observed stellar cluster spectra.

The theoretical, synthetic model spectra are created assuming all stars formed at the same time in a cluster following a Salpeter IMF. As the cluster ages, its stars evolve according to their initial masses. The evolution of the integrated spectrum reflects the overall changes occurring to the entire system of stars (the cluster) as a function of time. Therefore the shape and predominant spectral features of the integrated spectrum will uniquely change with the age of the cluster, ideally allowing a single age to be matched against an observed stellar cluster's spectrum.

The literature abounds with a large number of models used to produce synthetic spectra (Leitherer et al. 1999; Vazdekis 1999; Bruzual & Charlot 2003; Cervino & Luridiana 2006; Kotulla et al. 2009; Gonzalez Delgado et al. 2005). We chose the Gonzalez Delgado et al. (2005) model for our analysis.[4] We feel the Gonzalez Delgado et al. (2005) models are superior with regards to their treatment of lower mass stellar evolution tracks, as given by the Padova group. The Gonzalez Delgado et al. (2005) models are also available with relatively high resolution (0.3 Å). The stellar cluster model we are using assumes Salpeter (1955) initial mass function (IMF) with lower and upper cut-off masses of 0.1 and 120 solar masses, respectively. As we mentioned, the evolutionary model library used in the synthetic spectral calculations is the Padova asymptotic giant branch (AGB) stellar model for $Z = 0.008$, the metallicity for the much of the LMC. LMC clusters are known to have [Fe/H] values from -2.2 to 0.0 dex, or between -1.0 to 0.0 dex, for the age range we are using. Our analysis is done on spectra taken in the optical range. Bica & Alloin (1986) and Benítez-Llambay et al. (2012) have shown that metallicity does not play a significant role in the optical range when applying spectral aging methods. This is because optical lines are relatively insensitive to this level of change in metallicity. The stellar cluster sample in this work has ages <2 Gyr. Cole et al. (2005) show that for ages <5 Gyr most LMC clusters have a $[\mathrm{Fe/H}] = -0.4$.

[4] The model was obtained from http://www.iaa.es/~rosa/research/synthesis/HRES/ESPS-HRES.html.

4. THE METHOD

Our goal is to obtain the best match between the observed spectrum (corrected for a range of reddening values) and the synthesized model spectrum (for the range of ages available) to determine the cluster age and reddening. We will then compare the age derived via this spectral match against the age given in the literature based on a CMD analysis to tell us how well the spectral aging method worked.

First we smooth the model resolution to match our observed spectra. The model is further normalized at $\lambda = 5870$ Å as was done with our observed spectra.

We looked for the combination of age and reddening that minimizes the sum:

$$\chi^2 = \sum_{\lambda=3626\text{Å}}^{6230\text{Å}} \left(\frac{(\mathrm{OF})_\lambda - (\mathrm{MF})_\lambda}{(\mathrm{OF})_{5870\text{Å}}} \right)^2. \quad (1)$$

where OF is the observed flux and MF is the model flux. The observed flux is reddening corrected. This is done by applying the Cardelli et al. (1989) (CCM) extinction law in the optical range ($R = 3.1$). We use the range of reddening from 0.0 to 0.5, in steps of 0.01. While the age and reddening of a cluster are not physically correlated, they both affect the shape of the spectrum in a similar way. However, when combined with matching of the spectral features, this provides a sufficiently unique, single minima to break the age-reddening degeneracy that befalls broad-band photometric aging methods (Asa'd & Hanson 2012).

The combination of reddening-corrected observed spectrum and model spectrum (representing log[ages/year] from 6.60 to 10.25 in steps of 0.05) that minimizes equation (1) is taken as the reddening and age of the cluster. Figure 7 shows the results of the match found by this method for the cluster NGC1856 as an example.

Once this method is applied to the entire sample to determine age and extinction, we compare those results with the CMD ages. Table 4 shows the predicted age and reddening of our sample. The "Error" colum will be discussed in the next section. Figure 8 shows the correlation between our spectral ages and the literature CMD ages. Very good agreement is found, with

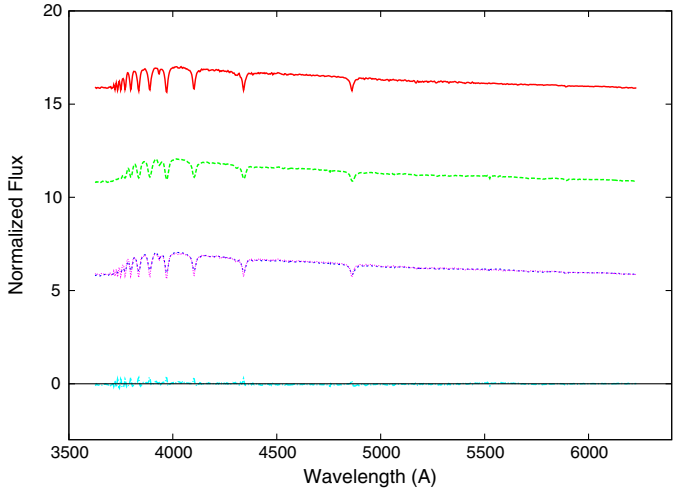

FIG. 7.—NGC1856—The top spectrum is the model spectrum of $\log(\text{age/year}) = 8.500$, the spectrum below that is the observed spectrum corrected for E(B-V) = 0.11. These two spectra were chosen as the best match as shown in the overlaid spectra near the center of the figure. The bottom of the figure shows the residuals of the above model spectrum and observed spectrum, that is (model spectrum)—(observed spectrum). The spectra are normalized at 5870 Å and shifted on the vertical axis for clarity. See the electronic edition of the *PASP* for a color version of this figure.

a correlation coefficient of 0.95. The vertical bars associated with the ages determined from integrated spectra represent the age step between the models used ($\log[\text{age/year}] = 0.05$) and does not represent a true error measure.

TABLE 4
AGE AND EXTINCTION FROM INTEGRATED SPECTRA

Name	Run	Age[a]	Error[b]	E(B-V)
NGC1711	Blanco	7.600	45%	0.08
NGC1856	Blanco	8.500	119%	0.11
NGC1903	Blanco	8.150	66%	0.05
NGC1984	Blanco	6.900	12%	0.04
NGC2011	Blanco	6.900	27%	0.00
NGC2156	Blanco	8.000	50%	0.00
NGC2157	Blanco	8.150	112%	0.05
NGC2164	Blanco	7.950	56%	0.00
NGC1651	SOAR	9.050	56%	0.00
NGC1850	SOAR	8.100	104%	0.00
NGC1863	SOAR	7.500	117%	0.09
NGC1983	SOAR	7.000	23%	0.00
NGC1994	SOAR	6.600	58%	0.18
NGC2002	SOAR	6.850	76%	0.29
NGC2031	SOAR	8.300	23%	0.00
NGC2065	SOAR	8.200	76%	0.03
NGC2155	SOAR	10.000	120%	0.00
NGC2173	SOAR	9.550	52%	0.00
NGC2213	SOAR	9.150	45%	0.00
NGC2249	SOAR	8.650	39%	0.00

[a] The unit is log(age/yr)
[b] Percentage Error. See eq. (2) in § 5.

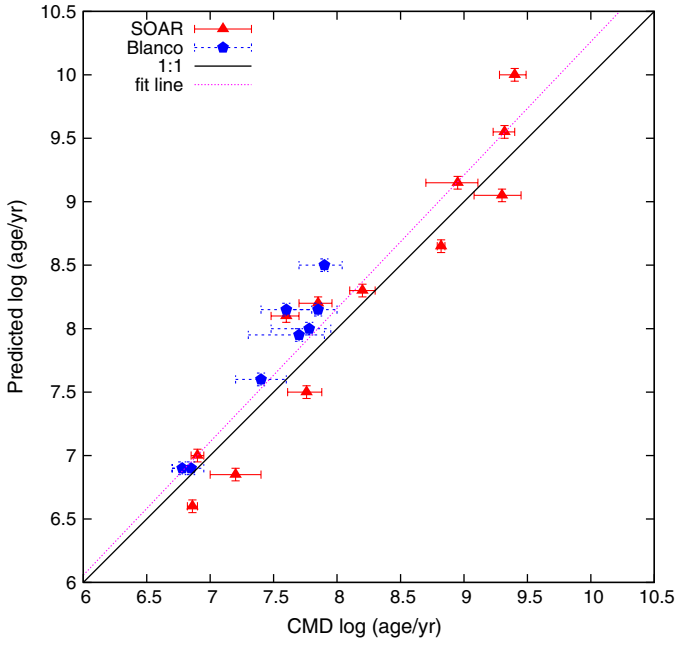

FIG. 8.—The correlation between our obtained ages and the literature CMD ages. The correlation coefficient is 0.95. The vertical bars associated with the ages determined from integrated spectra represent the age step between the models used ($\log(\text{age/year}) = 0.05$). See the electronic edition of the *PASP* for a color version of this figure.

Figure 9 shows the correlation between our E(B-V) and the literature E(B-V) values. We notice that the spectral aging method predicts values in an acceptable range of reddening for the LMC (<0.3).

5. MORE INTEGRATED SPECTRA FROM THE LITERATURE

To expand our sample, we will now apply our aging method to spectra available in the literature for seven additional LMC stellar clusters. Integrated spectra of four clusters are from Santos et al. (2006) and three clusters are from Palma et al. (2008). These spectra were kindly provided by the authors (in bins of 2 Å). The salient details of these clusters' properties are given in Table 5. In order to be consistent with the method used for our own spectra, we used the same wavelength range for the analysis of these spectra obtained from the literature. Table 6 presents the results of age and extinction determined for each cluster using the method presented in § 4.

As a means to estimate the uncertainty in our aging method, we have derived the percentage error for each stellar cluster in our sample using the equation:

$$\%\text{Error} = \left(\frac{|(\text{Age}_{\text{CMD}}) - (\text{Age}_{\text{predicted}})|}{(\text{Age}_{\text{Average}})}\right) \times 100. \qquad (2)$$

Here Age_{CMD} is the CMD age from the literature in years,

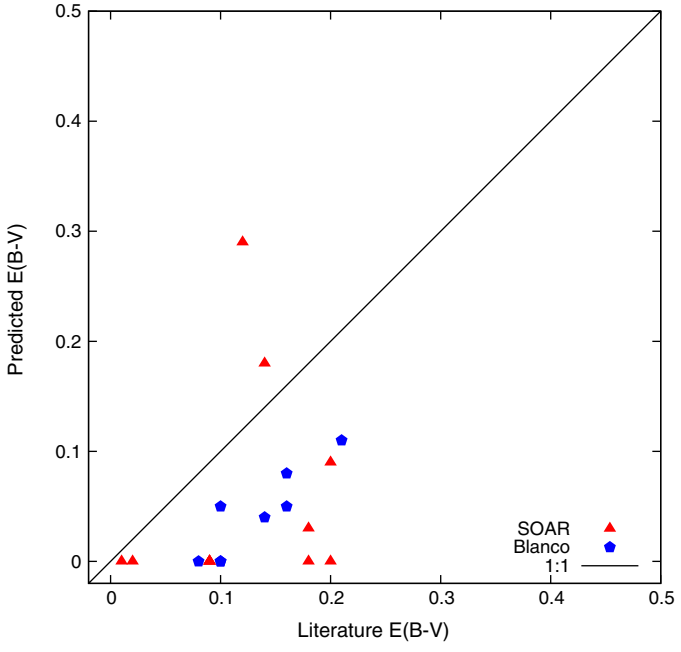

FIG. 9.—The correlation between our obtained E(B-V) and the literature E(B-V). Note that the predicted values lie in an acceptable range of reddening for the LMC (<0.3). See the electronic edition of the *PASP* for a color version of this figure.

$Age_{predicted}$ is the age obtained in this work in years and $Age_{Average}$ is the average of the CMD age and predicted age in years. These values are presented for each cluster in Tables 4 and 6. Figure 10 further illustrates the typical error seen in using our method for aging these clusters. The inner dotted lines represent a factor of 3 difference in CMD and predicted age, and the outer lines represent a factor of 10 difference.

6. THE TEMPLATES METHOD

Santos et al. (1995) and Piatti et al. (2002) formed a library of observations of stellar clusters with known age, reddening, and metallicity. This library was used to create models (templates) representing each age group. These templates can be used to estimate the age and reddening of unresolved stellar clusters using the χ^2 minimization method.

Benítez-Llambay et al. (2012) organized these templates by providing a user-friendly software (FISA) that makes it easy for the user to obtain the age of a star cluster from its observed optical integrated spectrum. We used FISA to get the ages of our observed sample of clusters; we used the combinations of age and reddening with the minimum χ^2 that has no negative E(B-V). Table 7 shows the results obtained. Note that most templates give a range of ages. The values listed are the log of the average of the age (in years) given by the templates.

Figure 11 shows the correlation between the ages obtained using FISA and the literature CMD ages. The correlation coefficient is 0.66. When excluding the outlier the correlation coefficient improves a bit to 0.80. The average percent error (see eq. [2] in § 5) is 103%, while the average percent error using our method is 69%.

7. DISCUSSION

In Paper 1 (Asa'd & Hanson 2012), we derived ages for 84 LMC stellar clusters by matching broad-band integrated photometry with colors predicted by simple stellar population models as a function of age. However, these photometric ages, compared to the previously reported CMD ages from the literature, showed only a weak correlation of 0.61. In several cases, older unreddened clusters were mistaken for more reddened young clusters. We also showed how this age - extinction degeneracy resulted in two or more minima (χ^2) solutions for several clusters.

In this new work we examine if integrated spectra will provide better predictions of the age of clusters. Out of that original sample of 84 clusters, we now have integrated spectra of 27 clusters. For a fair comparison between the aging method using integrated photometry and the aging method using integrated spectra we show the results of ages obtained with both methods for this particular subsample of 27 clusters in common in Figure 12. Figure 13 shows the reddening results obtained with both methods for this shared subsample of 27 clusters.

TABLE 5
SPECTRA OBTAINED FROM THE LITERATURE

Name	Source	Resolution (Å)	Mass[a]	Age[b]	Ref.	E(B-V)	Ref.
NGC1839	Santos et al. (2006)	14	2	7.52	Alcaino & Liller (1987)	0.27	Alcaino & Liller (1987)
NGC1870	Santos et al. (2006)	14	3	7.86	Alcaino & Liller (1987)	0.14	Alcaino & Liller (1987)
NGC1894	Santos et al. (2006)	14	3	7.74	Dieball et al. (2000)	0.1	Dieball et al. (2000)
SL237	Santos et al. (2006)	14	2	7.43	Alcaino & Liller (1987)	0.17	Alcaino & Liller (1987)
NGC2136	Palma et al. (2008)	17	3	7.60	Hodge (1983)	0.10	Persson et al. (1983)
NGC2172	Palma et al. (2008)	17	2	7.78	Hodge (1983)	0.1	Persson et al. (1983)
SL234	Palma et al. (2008)	17	2	7.68	Alcaino & Liller (1987)	0.15	Alcaino & Liller (1987)

[a] See the text for details about the mass ranges represented by these numbers.
[b] These are the CMD ages obtained from the literature. The unit is log(age/yr).

TABLE 6
AGE AND EXTINCTION FROM INTEGRATED SPECTRA

Name	Source	Age[a]	Error[b]	E(B-V)
NGC1839	Santos06	8.100	117%	0.00
NGC1870	Santos06	8.050	43%	0.00
NGC1894	Santos06	8.150	88%	0.15
SL237	Santos06	6.850	117%	0.17
NGC2136	Palma08	8.150	112%	0.04
NGC2172	Palma08	6.800	162%	0.03
SL234	Palma08	7.700	5%	0.06

[a] The unit is log(age/yr).
[b] Percentage Error. See eq. (2) in § 5.

In Paper 1, we showed that using integrated photometry to determine age through χ^2 minimization to model colors is tricky due to the age-reddening degeneracy. UBV colors of older clusters with low E(B-V) will appear similar to young clusters with high E(B-V). Luckily, this is not the case when using integrated spectra. As an example, consider the cluster NGC2173. The CMD log(age/year) is 9.32 (Mould et al. 1986b) and the predicted log(age/year) from integrated spectroscopy is 9.55. But the predicted age from integrated photometry is 7.75. The literature extinction for this cluster is 0.14 (Mould et al. 1986b). The predicted extinction from integrated spectroscopy is 0.00 while the predicted extinction from integrated photometry is 0.78. When one looks at the two model spectra in Figure 14 the overall slope, captured by broad-band photometry, looks very similar, but the spectral features are quite different. When comparing these two model spectra to a real cluster spectrum, there will be no ambiguity which is the correct match provided the spectra has sufficiently high resolution.

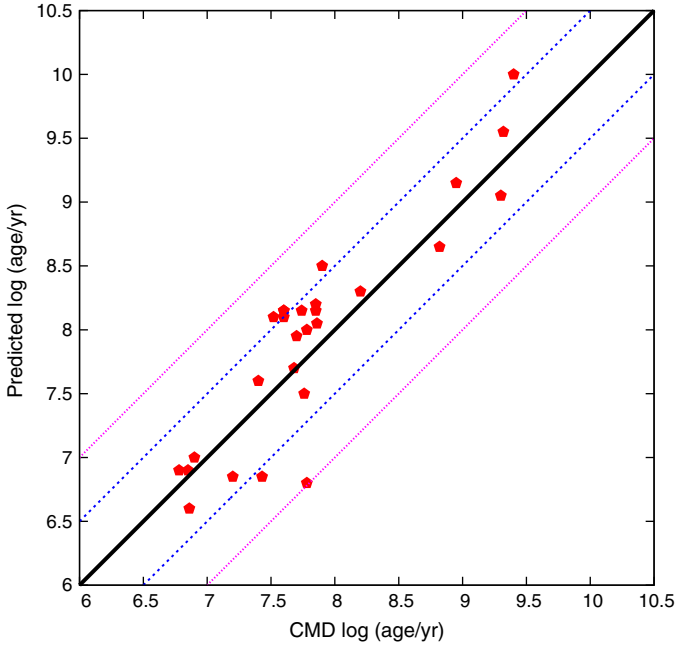

FIG. 10.—Uncertainty in our age prediction. The inner lines represent a factor of 3 difference in age, and the outer lines a factor of 10 difference in age. See the electronic edition of the *PASP* for a color version of this figure.

TABLE 7
AGE AND EXTINCTION FROM TEMPLATES

Name	Best matching template[a]	Age[b]	Error[c]	E(B-V)
NGC1651	Yg	8.44	151%	0.14
NGC1711	Yb3	6.48	157%	0.18
NGC1839	Yf	8.10	117%	0.00
NGC1850	Yb3	6.88	136%	0.20
NGC1856	Yg	8.44	110%	0.16
NGC1863	Yb1-WR-SG	6.88	153%	0.33
NGC1870	Yb3	6.88	162%	0.22
NGC1894	Yg	8.44	133%	0.09
NGC1903	Ye	7.78	16%	0.06
NGC1983	Ya3-WR	6.65	56%	0.20
NGC1984	Ya3-WR	6.65	45%	0.45
NGC1994	Ya3	6.48	82%	0.42
NGC2002	Ya3-WR	6.65	112%	0.80
NGC2011	Ya3-WR	6.65	30%	0.44
NGC2031	Ye	7.78	90%	0.01
NGC2065	Ye	7.78	16%	0.05
NGC2136	Ye	7.78	41%	0.06
NGC2155	Ia	9.00	86%	0.03
NGC2156	Yb3	6.88	155%	0.22
NGC2157	Ye	7.78	41%	0.05
NGC2164	Yb3	6.88	147%	0.16
NGC2172	Yb3	6.88	155%	0.25
NGC2173	Yb3-WR-SG	6.88	199%	0.92
NGC2213	Yh	8.70	56%	0.08
NGC2249	Yg	8.44	82%	0.08
SL234	Yb3	6.88	145%	0.18
SL237	Yb2	6.88	112%	0.47

[a] Refer to Benítez-Llambay et al. (2012) for details about these templates.
[b] The unit is log(age/yr). Note that the templates don't give an exact age, but rather a range (in years). The values shown here are the log of the average of the age given by the templates.
[c] Percentage Error. See eq. (2) in § 5.

One concern to keep in mind is the variation of spectral properties expected to be seen from integrated spectra of low- and intermediate-mass stellar clusters. This is due to the small number of stars populating the highest current mass bin, creating stochastic sampling effects. This can be quite strong particularly in younger clusters with $\log(\mathrm{age}) < 8.0$ (Cervino & Luridiana 2004, 2006). Moreover, our synthetic spectra come from models that make no correction for these variations. In fact, for young, low-mass clusters, they are not even *able* to match these synthetic spectra, as it would require flux from the highest mass stars to originate from statistically predicted, but nonphysical, fractional stars. For this reason, we expect age predictions based on spectra for the lowest mass clusters would not fit as well as with our more massive stellar clusters.

Such concerns are not supported by our results. Figure 15 shows that for our sample of 27, there is no significant trend in the accuracy of age estimates based on cluster mass. The

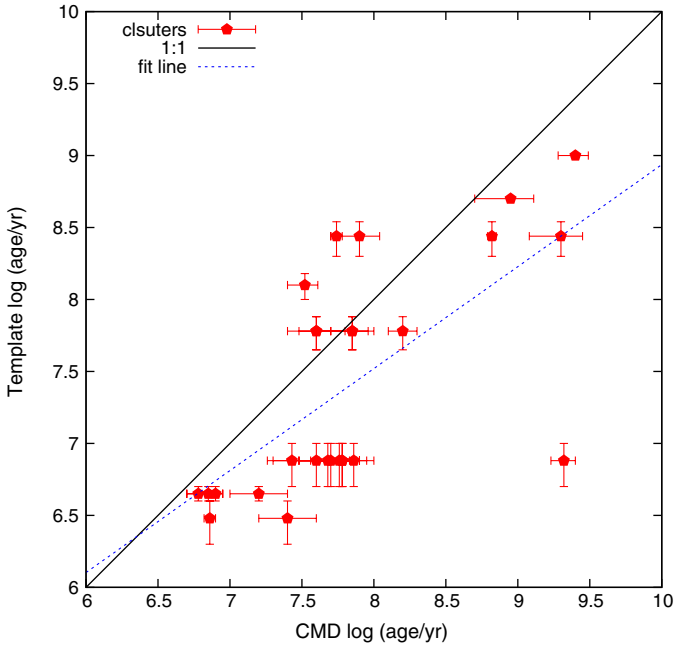

FIG. 11.—The correlation between the ages obtained using FISA and the literature CMD ages. The correlation coefficient is 0.66. See the electronic edition of the *PASP* for a color version of this figure.

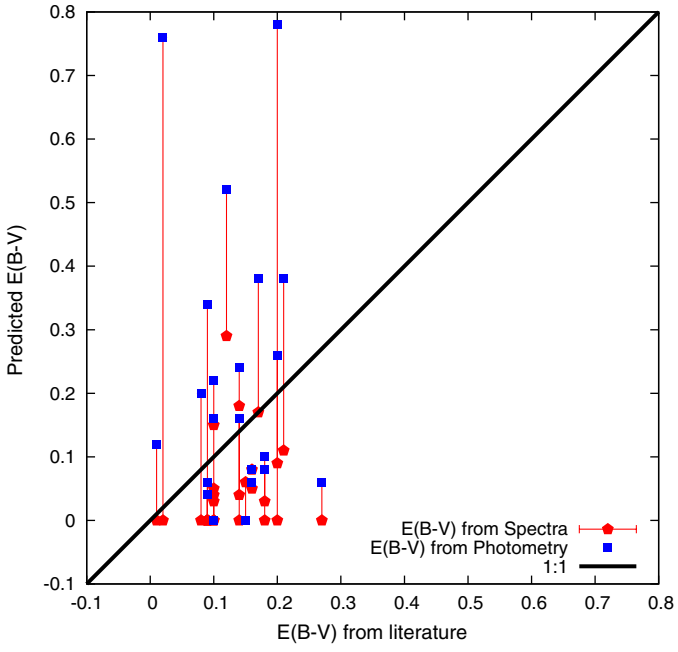

FIG. 13.—The correlation between the extinction obtained from integrated photometry (*blue squares*) or integrated spectra (*red pentagons*) for the current subsample. The values for the same cluster is connected by a vertical line. See the electronic edition of the *PASP* for a color version of this figure.

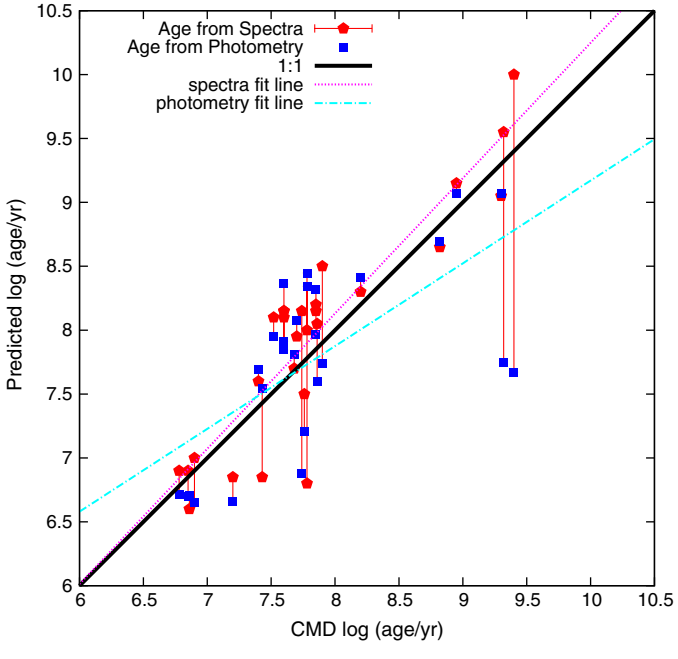

FIG. 12.—The correlation between the ages obtained from integrated photometry (*blue squares*) or integrated spectra (*red pentagons*) and CMD ages for the shared subsample. The values of the same cluster are connected by a vertical line. The correlation coefficient of age for this subsample with integrated photometry is 0.67. See Asa'd & Hanson (2012) for a discussion of the age analysis. The correlation coefficient for aging based on integrated spectra for this subsample is 0.90. See the electronic edition of the *PASP* for a color version of this figure.

numbers from 1 to 5 represent the different mass categories, from lowest to highest (see § 1). Although the sample is rather small and cannot be used to argue that no mass-effect exists when using integrated spectra to obtain age, our aging method

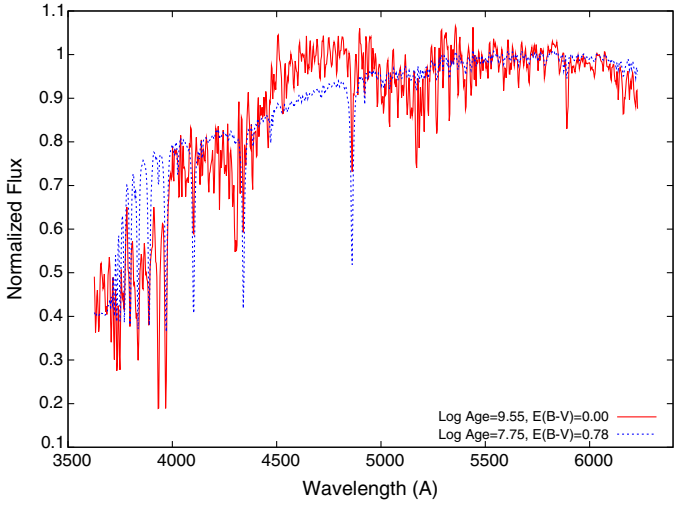

FIG. 14.—Synthetic spectrum of a cluster of $\log(\text{age/year}) = 9.55$ with $E(B\text{-}V) = 0.0$, the closest match to the properties obtained from integrated spectra for the cluster NGC2173, and another one with $\log(\text{age/year}) = 7.75$ with $E(B\text{-}V) = 0.78$, representing the information predicted by the integrated photometry method for this cluster. The method of integrated spectra can better break the age-extinction degeneracy. See the electronic edition of the *PASP* for a color version of this figure.

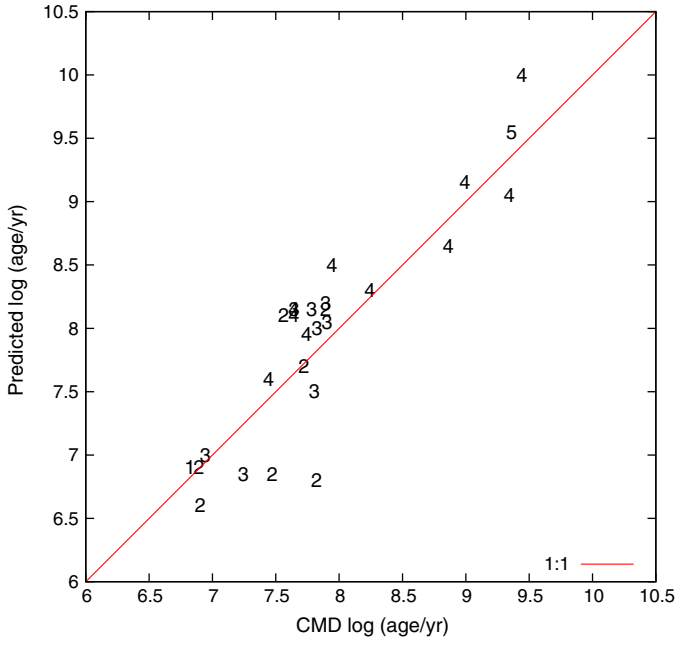

FIG. 15.—Numbers from 1 to 5 represent the different mass categories (see § 1). Category 1 represents clusters with masses from 1,000 to $3,750\ M_{\odot}$. Category 2 represents clusters with mass from 3,750 to $10,000\ M_{\odot}$ Category 3 represents clusters with masses between 10,000 and $25,000\ M_{\odot}$. Category 4 represents clusters with masses between 25,000 and $100,000\ M_{\odot}$. Category 5 represents clusters with masses between 100,000 and $250,000\ M_{\odot}$. For this small sample there is no significant difference in the accuracy of the spectral aging with cluster mass. See the electronic edition of the *PASP* for a color version of this figure.

comparing with a synthetic spectrum, appears to work equally well with low-, intermediate- and high-mass clusters.

8. SUMMARY

The importance of having accurate aging techniques in astronomical investigations can not be overstated. Stellar clusters are still among the most heavily used astronomical chronometers, being important for both Galactic and extragalactic work. In this contribution we have amassed spectra, most newly obtained, but some taken from the literature, for 27 LMC stellar clusters with previously determined CMD ages and extinctions. We have investigated the most commonly used method for aging unresolved stellar clusters, through matching their integrated spectra with modern synthesized model spectra. Overall, we find very good agreement, with nearly all stellar cluster ages matching within a factor of 4. For the clusters with new high resolution spectra obtained by us, all but three match the CMD ages within a factor of $\approx$2.

We summarize our work in the following points:

1. We test the method of obtaining ages of unresolved stellar clusters from integrated spectra by comparing those predictions with the known CMD ages and found a good correlation.
2. We demonstrate that using integrated spectra and a full spectrum model fitting is a better age estimator than using just integrated photometry.
3. We show that aging methods using integrated spectra does not suffer the same age—extinction degeneracy seen when aging clusters based on integrated photometry (Asa'd & Hanson 2012).
4. We observe no significant difference in the accuracy of ages derived using integrated spectra with intrinsic mass of the stellar clusters.

We wish to thank the referee who provided valuable suggestions and corrections that greatly improved the presentation of our results. We thank Nidia Morrell for helping establishing the collaboration of this work. We acknowledge Mario Hamuy for assistance with the flux calibration. J. F. C. Santos, Roberto Cid Fernandes and Claus Leitherer provided useful comments. We thank the staff at CTIO and SOAR for their valuable help and guidance. This work was supported in part by the National Science Foundation under Grant No. AST-1009550 to the University of Cincinnati, P.I., M. Hanson and Grant No. PHY-0855860 to the University of Cincinnati, P.I., M. Sokoloff. NOAO sponsored the first author's travels to Blanco and SOAR.

REFERENCES

Alcaino, G., & Liller, W. 1987, AJ, 94, 372
Asa'd, R. S., & Hanson, M. M. 2012, MNRAS, 419, 2116
Beasley, M. A., Hoyle, F., & Sharples, R. M. 2002, MNRAS, 336, 168
Benítez-Llambay, A., Clariá, J. J., & Piatti, A. E. 2012, PASP, 124, 173
Bica, E., & Alloin, D. 1986, A&A, 162, 21
———. 1987, A&A, 186, 49
Bica, E., Alloin, D., & Schmitt, H. R. 1994, A&A, 283, 805
Bica, E., Santos, J. F. C., & Alloin, D. 1990, A&A, 235, 103
Bruzual, G., & Charlot, S. 2003, MNRAS, 344, 1000
Cardelli, J. A., Clayton, G. C., & Mathis, J. S. 1989, ApJ, 345, 245
Cervino, M., & Luridiana, V. 2004, A&A, 413, 145
———. 2006, A&A, 451, 475
Cid Fernandes, R., & Gonzalez Delgado, R. M. 2010, MNRAS, 403, 780
Cole, A. A., Tolstoy, E., Gallagher, J. S., III, & Smecker-Hane, T. A. 2005, AJ, 129, 1465
Da Costa, G. S., Mould, J. R., & Crawford, M. D. 1985, ApJ, 297, 582
Dieball, A., Grebel, E. K., & Theis, C. 2000, A&A, 358, 144
Dirsch, B., Richtler, T., Gieren, W. P., & Hilker, M. 2000, A&A, 360, 133
Elson, R. A., & Fall, S. M. 1988, AJ, 96, 1383
Elson, R. A. W. 1991, ApJS, 76, 185
Gonzalez Delgado, R. M., Cerviño, M., Martins, L. P., Leitherer, C., & Hauschildt, P. H. 2005, MNRAS, 357, 945
Hamuy, M., Suntzeff, N. B., Heathcote, S. R., et al. 1994, PASP, 106, 566

Hamuy, M., Walker, A. R., Suntzeff, N. B., et al. 1992, PASP, 104, 533
Hodge, P. W. 1983, ApJ, 264, 470
———. 1984, PASP, 96, 947
Jones, J. H. 1987, AJ, 94, 345
Kerber, L. O., Santiago, B. X., & Brocato, E. 2007, A&A, 462, 139
Koleva, M., Prugniel, P., Ocvirk, P., Le Borgne, D., & Soubiran, C. 2008, MNRAS, 385, 1998
Kotulla, R., Fritze, U., Weilbacher, P., & Anders, P. 2009, MNRAS, 396, 462
Leitherer, C., Schaerer, D., Goldader, J. D., et al. 1999, ApJS, 123, 3
Lejeune, T., & Schaerer, D. 2001, A&A, 366, 538
Leonardi, A. J., & Rose, J. A. 2003, AJ, 126, 1811
Marigo, P., Girardi, L., Bressan, A., et al. 2008, A&A, 482, 883
Meurer, G. R., Freeman, K. C., & Cacciari, C. 1990, AJ, 99, 1124
Mould, J. R., Da Costa, G. S., & Crawford, M. D. 1986a , ApJ, 304, 265
Mould, J. R., Da Costa, G. S., & Wieland, F. P. 1986b , ApJ, 309, 39
Palma, T., Ahumada, A., Claria, J., & Bica, E. 2008, Astron. Nachr., 329, 392
Persson, S. E., Aaronson, M., Cohen, J. G., Frogel, J. A., & Matthews, K. 1983, ApJ, 266, 105
Piatti, A. E., Santos, J. F. C., Clariá, J. J., et al. 2005, A&A, 440, 111
Piatti, A. E., Sarajedini, A., Geisler, D., Bica, E., & Claria, J. J. 2002, MNRAS, 329, 556
Popescu, B., & Hanson, M. M. 2010, ApJ, 713, L 21
Salpeter, E. E. 1955, ApJ, 121, 161
Santos, J. F. C., Bica, E., Claria, J. J., et al. 1995, MNRAS, 276, 1155
Santos, J. F. C., Claria, J. J., Ahumada, A. V., et al. 2006, A&A, 448, 1023
Talavera, M., Ahumada, A., Santos, J., et al. 2010, Astron. Nachr., 331, 323
Trancho, G., Bastian, N., Miller, B. W., & Schweizer, F. 2007, ApJ, 664, 284
Vallenari, A., Bettoni, D., & Chiosi, C. 1998, A&A, 331, 506
Vazdekis, A. 1999, ApJ, 513, 224
Wolf, M. J., Drory, N., Gebhardt, K., & Hill, G. J. 2007, ApJ, 655, 179
Worthey, G., & Ottaviani, D. L. 1997, ApJS, 111, 377